

UDC 681.782.473:615.47

S.V. PAVLOV, T.I. KOZLOVSKAYA

Vinnitsia National Technical universitet, Vinnitsa, Ukraine

R.H. ROVIRA

UPSE «Universidad Peninsula de Santa Elena», Ecuador

SENESCYT «Ministry of Higher Education, Science, Technology and Innovation», Ecuador

DESIGN AND AUTOMATION OF A VIDEOPOLARIMETRY SYSTEM FOR THE ANALYZING OF THE POLARIZATION PROPERTIES OF A BIOLOGICAL SAMPLE

Nowadays, the use of the polarimetry techniques for display and study of biological tissues has gained increasing interest. This interest is related mainly to the non-invasiveness, relatively low cost, and ease of application among other characteristics. For full use of these advantages, the automation of systems is required. In this paper presents development a layout and a new method for automation of mapping the bi-dimensional polarization properties of biological tissues.

Key words: videopolarimetry system, distribution of polarization properties, Stokes parameter, Mueller matrix.

С.В. ПАВЛОВ, Т.И. КОЗЛОВСКАЯ

Винницкий национальный технический университет, Винница, Украина

Р.У. РОБИРА

UPSE «Universidad Península de Santa Elena», Эквадор

SENESCYT «Министерство высшего образования, науки, технологий и инноваций», Эквадор

АРХИТЕКТУРА И МЕТОД АВТОМАТИЗАЦИИ ВИДЕОПОЛЯРИМЕТРА ДЛЯ АНАЛИЗА ПОЛЯРИЗАЦИОННЫХ СВОЙСТВ БИОЛОГИЧЕСКОГО ОБРАЗЦА

В настоящее время использование поляриметрии для визуализации и исследования биологических тканей получило большой интерес. Это связано в основном с неинвазивностью, относительно низкой стоимостью и легкостью применения в сравнении с другими методами. Для полного использования этих преимуществ, требуется автоматизация существующих приборов. В данной статье представлена разработка архитектуры и нового метода для автоматизации картирования двумерного распределения поляризационных свойств биологических тканей.

Ключевые слова: видеополяриметрия системы, распределения поляризационных свойств, параметр Стокса, мюллера матрица.

Introduction

The propagation of light in biological tissues (BT) depends on the scattering and absorption properties of its components. Therefore, from the characteristics of the scattered light it can be concluded about changes in structure, shape or size of such components. Hence optical methods (OM) have a special place among research and imaging techniques for diagnosis of the structures of BT. Among the main advantages of OM, there may be pointed out the high information content, multifunctional nature of their applications, the relative simplicity and low cost of implementation.

Recently, there has been a growing interest in methods based on the polarization properties. The analysis of polarization of the scattered radiation provides different results for the analysis of morphological and functional state of BT. These results serve as a basis for the development of new diagnostic systems [1-4]. A promising direction of videopolarimetry for diagnosis of biological samples is the development of automated systems. Today, a number of research organizations develop such systems [5].

Automated video polarimetry [5] system together with image processing techniques successfully implements methods for determining the polarization characteristics of anisotropic tissues. These systems allow obtaining the values of azimuth, ellipticity and phase shift of scattered light for each pixel in the acquired image. However, experimental methods and the technical implementation are very specialized, which leads to the lack of a unified information base. This drawback prevents the standardization of processes. Therefore, the development of a multi-functional, complex automated videopolarimetry system for the study of BT with a thorough analysis of the data is a matter of scientific interest. Such a system would improve the diagnostic reliability of the structure of biological samples.

The **objective of this work** is to improve the layout and algorithm of a videopolarimetry system with enhanced functionality that implements the methods of Stokes and Mueller mapping of biological tissue samples, complemented with the estimation of the systematic error in order to improve reliability of diagnosis.

Methodology

The Stokes vector parameters S_i are obtained on the basis of six measurements of light fluxes with different polarization states. The different states are obtained when light passes through appropriate combinations of optics components. Figure 1 depicts the disposition and angular orientation of the phase plates, polarizers, analyzers that comprise the system.

The layout of the automated video polarimetry system includes a light source LS, a collimator CL, a linear polarization filter LP1, a non polarizing beam splitter prism BS, a quarter-wave plate WP, a projection block F, an analyzer LP2 and a CCD camera.

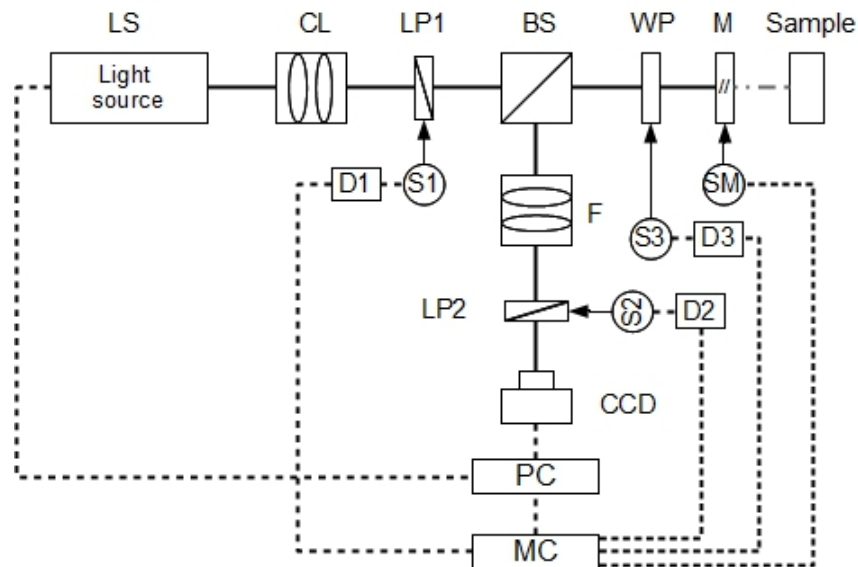


Figure 1: The layout of an automated videopolarimetry system. LS – light source, CL- collimator, LP – linear polarizer, BS – beam splitter, WP – quarter-wave plate, M – mirror, F – projection block, S – stepper motor, SM – selector, D – driver, CCD – camera, PC – computer, MC – micro controller.

The polarizing elements LP1 and WP allow changing the azimuth α , the ellipticity β , and the phase shift δ of the probing beam. This change is accomplished by rotation of LP1 within $[0^\circ < \varphi < 180^\circ]$ and the quarter-wave $(-45^\circ < \chi < 45^\circ)$. In this way, the biological sample can be probed with light of required polarization. The beam splitter has a twofold function. First it directs the light to the WP and the sample; and second guides the light toward the projection Block F, which in turn redirects the beam to the focal plane of the camera.

The analysis of the light scattered by the sample is carried out by the WP and the polarization filter LP2. The filtration process allows to determine the intensity distribution $I(\alpha, \beta)$ of images of the sample. The images are transmitted to the computer PC through the CCD camera. The acquired information $I(m \times n)$ is stored for the further calculation of the Stokes parameters $S_i(m \times n)$, azimuth $\alpha(m \times n)$, ellipticity $\beta(m \times n)$ and phase shifts $\delta(m \times n)$ distributions, where $m \times n$ is the size of the image.

The angular position of the polarization elements is controlled by a micro controller MC. The exchange of information between the computer program and the micro controller is carried out in specialized software. The principal function of MC is to govern the rotation of the stepper motors S1 – S3 through drivers D1 - D3. The following algorithm depicts the process of calibration and information acquisition.

Algorithm for obtaining and analyzing the polarization properties of a biological sample

1. System parameters determination
 - 1.1. generation of Stokes vectors S_i^{in} ; based on given values of azimuth α_i and ellipticity β_i
 - 1.2. calculation of the angular position of the polarization state generator PSG optical elements, φ_i, χ_i
2. Acquisition of data:
 - 2.1. for $i = 1$ to the number of records p
 - 2.1.1. Calibration of PSG for measurement i :
 - 2.1.1.1. placement of the mirror in the optical path,
 - 2.1.1.2. acquisition of the image of the scene,
 - 2.1.1.3. conversion of the image to grayscale,
 - 2.1.1.4. determination of the average value of pixels intensity in the image,
 - 2.1.1.5. passing to MC step motors SP1 and SP2.
 - 2.1.2. Determination of the output Stokes vector S_{out}^{in} for the input S_i^{in} :
 - 2.1.2.1. for $j = 1$ to the number of measurements r
 - 2.1.2.1.1. determination of the angular position ψ_j of analyzer LP2 for the minimization of the condition number κ of the modulation matrix MA,
 - 2.1.2.1.2. passing ψ_j to the step motor driver SP3.
 - 2.1.2.1.3. Removal of mirror from the optical path,
 - 2.1.2.1.4. Recording of the scene of the sample, for the positions ψ_j
 - 2.1.2.1.5. end
 - 2.1.2.2. Determination of S_i^{out} using the method of least squares
 - 2.1.2.3. Stokes vector $S^{out}(m \times n)$ is stored for further processing.
3. Processing of polarized information
 - 3.1. determination of the bi-dimensional distributions $\alpha(m \times n)$, $\beta(m \times n)$, $\delta(m \times n)$ of the sample
 - 3.2. Statistical and fractal analysis.

The role of the PSG is to create a modulation matrix which produces the appropriate polarization of probe light while ensuring effective levels of intensity in the detector. For this purpose, it is required to generate at least four distinct states of polarization through the Poincare sphere with high repeatability. A complete generator can create a beam of any polarization state. However, for this purpose, a set of wave plates is required, thereby increasing the cost and complexity of the installation. In the simplified PSG used in this work, to control the azimuth and ellipticity of the polarization ellipse is necessary to adjust the values of angle orientation of the linear polarizer and the quarter wave plate ϕ and χ respectively. Figure 2 shows the scheme of the proposed generator.

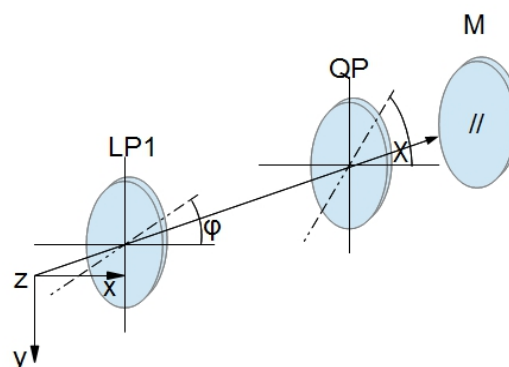


Figure 2: PSG scheme. Illustration of the angles for the setup of the PSG with a rotating quarter-wave plate and a linear polarization filter. The angle of the LP transmission axis and the angle of the fast axis of the QWP are denoted by ϕ and θ , respectively.

The Stokes parameters of the light after passing the PSG are given by the matrix multiplication:

$$S_{out} = Rot(\theta) * MQWP(0^0) * Rot(-\theta) * MLP(\phi) * S_{in}; \quad \phi \in \{0^0, 180^0\}; (-45 \leq \theta \leq 45^0) \quad (1)$$

where, MLP indicates the Mueller matrix of the linear polarizer, MQWP – the Mueller matrix of the quarter wave plate and Rot – the rotation matrix. Equation 1 can be written in canonical form in the following way:

$$S_{out} = \begin{bmatrix} 1/4 \\ \frac{\cos(2*\phi - 4*\chi) + \cos(2*\phi)}{8} \\ \frac{-\sin(2*\phi - 4*\chi) - \sin(2*\phi)}{8} \\ \frac{-\sin(2*\phi - 2*\chi)}{4} \end{bmatrix} \quad (2)$$

For the calibration of the generator, a mirror is positioned in the optical path. When circularly polarized light is reflected by the specular surface, it reverses helicity. As the reflected beam passes back through quarter wave plate the transmitted beam becomes linearly polarized, but now in the orthogonal directions to the first polarization direction. The back scattered beam reverses helicity again, passing through the non-polarizing beam splitter, which acts on this occasion as an attenuating mirror.

Results

A comparison of the proposed generator with a generator comprising a fixed quarter-wave plate a rotating linear polarizer and a fixed quarter wave plate (PLS+FQWP+RLP+FQWP) was performed. The criteria considered were: the ability to generate states of polarization with arbitrary azimuth and ellipticity, ease of generating base states of polarization I(0), I(90), I(45), I(135), I(L), I(R); and the deviation from the calculated values when an offset is introduced to the angular position of the optic elements.

The comparison was performed by simulating generator in Matlab. Figure 3 shows that in both cases the states of polarization are conditioned to the fact that the difference between the azimuth and ellipticity does not exceed 45. The hatched area represents the graphics generation capacity polarization states. As noted generator the proposed exceeds the compared one.

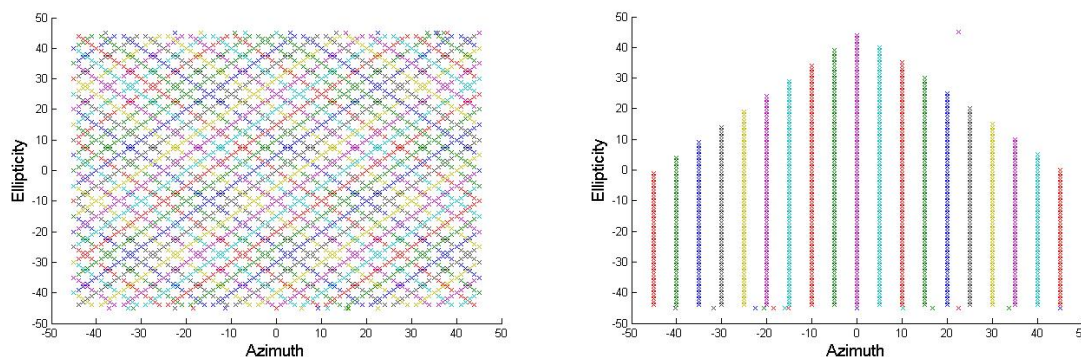


Figure 3: Generation of polarization with arbitrary azimuth and ellipticity. a) proposed PSG, b) PLS+FQWP+RLP+FQWP

Degenerate polarization states are shown in Figure 4. Unlike generator with two phase plates, these states are obtained for various combinations of angular positions χ and ϕ .

For the assessment of the effect of systematic angular deviations in the generation of polarization state, a constant value is added to the angle position of one of the optical elements. For the proposed generator the increase is added to the rotation of the wave-plate, while that for the generator compared to the rotation of the linear polarizer

added. The resulting deviation is expressed in relative terms with respect to module incident Stokes vector. Figure 5 shows the relative error for both cases. It was found that for the proposed case the relative error reaches a maximum value of 1.8 for a deviation of 1 degree in the rotating element, while for the case b this value reached 2.4.

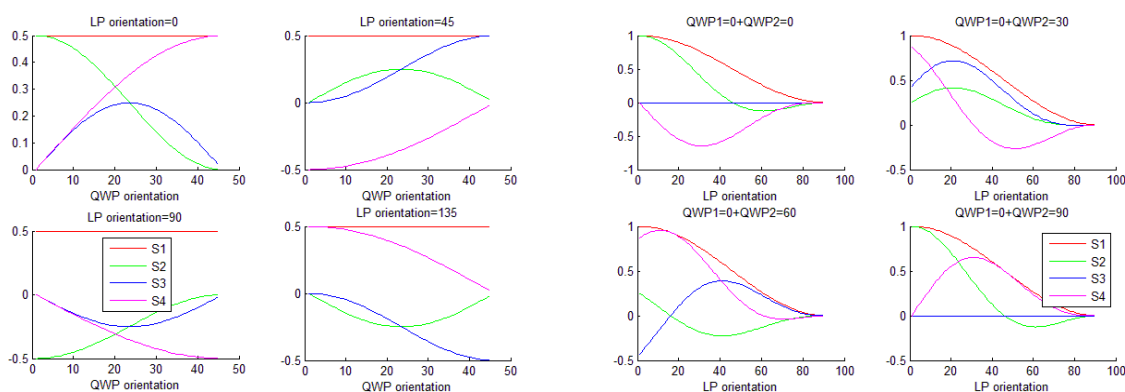


Figure 4: Degenerate polarization states a) proposed generator, b) PLS+FQWP+RLP+FQWP

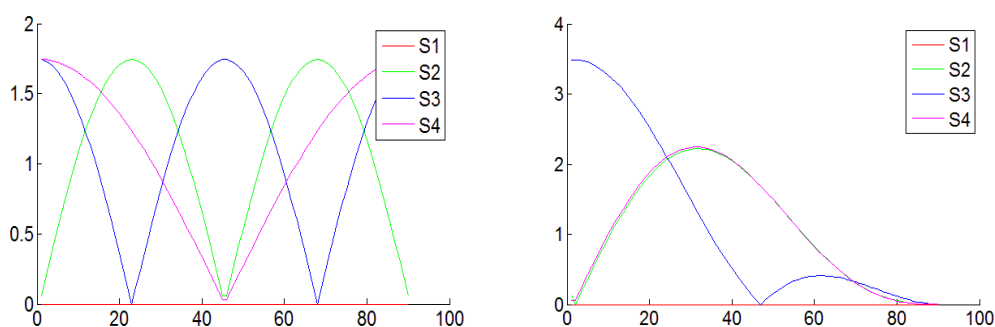


Figure 5: Relative error: a) Proposed generator, b) PLS+FQWP+RLP+FQWP

Conclusions

An enhanced layout and a new method for automation of mapping the bi-dimensional polarization properties of biological tissues were developed. In addition, a comparison of the polarization states generator of the proposed layout was performed. It was found, that the proposed generator can cover a wide range of azimuth and ellipticity, while minimizing optics and rotation elements. Additionally, it is less sensitive to systematic errors. One important advantage is that the intensity of the probed beam keeps constant for all combination of PSG. The proposed automation and calibration process improves the accuracy of calculation of phase shifts of laser images of optically thin biological layer through the registration of intensity beam that passed through a sample when crossed phase filters. This improvement was due to new methods of reconstruction of images of the layer structure of biological tissue and statistical, correlation and fractal analysis of the images.

Acknowledgments

This work was supported by the grant "The Ministry of Higher Education, Science, Technology and Innovation" SENESCYT "Ecuador, and is sponsored by the University of Santa Elena" UPSE ", Ecuador.

References

1. Cordo M., Sendra J. R., Viera A., Silva S. L. Diffuse reflectance spectroscopy of human skin lesions European Conference on Biomedical Optics. In European Conference on Biomedical Optics 2005. –P. 58620d – 58620d. International Society for Optics and Photonics.
2. Garcia-Urbe A. In vivo diagnosis of melanoma and nonmelanoma skin cancer using oblique incidence diffuse reflectance spectrometry / A. Garcia-Urbe, A., Zou, J., Duvic, M., Cho-Vega, J. H., Prieto, V. G., & Wang, L. V. // Cancer research. – 2012. – Vol. 72, № 11. – P. 2738–2745.
3. Kondepati V.R. Heise H.M. & Backhaus J. Recent applications of near-infrared spectroscopy in cancer diagnosis and therapy Analytical and bioanalytical chemistry. – 2008. – Vol. 390, № 1. – P. 125–139.
4. Tuchin V. Optical clearing of tissues and blood. – Bellingham: SPIE Press, 2006.
5. Zabolotna N. I. Architecture and algorithm of two-dimensional and analysis laser systems polarimetry biological tissue. Optoelectronic information and communication technology. - 2013. - № 1. - P. 54-65
6. Sundarapandian V. Numerical Linear Algebra PHI Learning Pvt. Ltd., 2008. – 620 p.